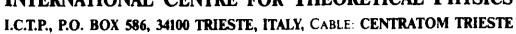
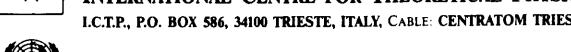


UNITED NATIONS EDUCATIONAL, SCIENTIFIC AND CULTURAL ORGANIZATION INTERNATIONAL CENTRE FOR THEORETICAL PHYSICS









UNITED NATIONS INDUSTRIAL DEVELOPMENT ORGANIZATION

INTERNATIONAL CENTRE FOR SCIENCE AND HIGH TECHNOLOGY C/O INTERNATIONAL CENTRE FOR THEORETICAL PHYSICS 34100 TRIESTE (ITALY) VIA GRIGNANO, 9 (ADRIATICO PALACE) P.O. BOX 586 TELEPHONE 040-234572 TELEFAX 040-234575 TELEX 46049 APH I

SMR/760-25

"College on Atmospheric Boundary Layer and Air Pollution Modelling" 16 May - 3 June 1994

"Mass-Consistent Models for Wind Fields over Complex Terrain: the State-of-the-Art"

> C. RATTO Department of Physics University of Genoa Genoa, Italy

Please note: These notes are intended for internal distribution only.



MASS-CONSISTENT MODELS FOR WIND FIELDS OVER COMPLEX TERRAIN: THE STATE OF THE ART*

C.F. Ratto, R. Festa, C. Romeo
Department of Physics, University of Genoa, Genoa, Italy
and
O.A. Frumento[†], M. Galluzzi
ITA.12, Genoa, Italy

ABSTRACT

Among the diagnostic models for wind field simulation, mass-consistent models play an important role, thanks to the simplicity of the physics involved and their capacity to accept several measurements of wind at different points of the domain. The general procedure and mathematical supports for this kind of simulation, with particular reference to the approximations that characterize the different models developed, are analysed. Evidently, a large number of simulations is required if one needs to know the average wind over a region, with a consequent long calculation time. Some methods reducing this time, without losing fundamental information, are described.

KEY WORDS

Mass-consistent wind field, diagnostic wind models, comparison of models, review paper.

INTRODUCTION

The knowledge of the three-dimensional wind field over a region is often required for a large number of applications: evaluation of energy obtainable from Wind Energy Converter Systems (WECS), simulation of wind action on structures (buildings, bridges, etc.), transport and diffusion of pollutants and development of forest fires. Correctly modelled 3-D wind fields could also be useful for formulating initial and boundary conditions required by mesoscale dynamical models.

Furthermore, as noted by Kitada et al. [1], it is extremely important to know the vertical wind field in order to reliably predict the transport of air pollutants. Limited horizontal wind mesurements are usually available, and these are affected by intrinsic errors which make estimation of the vertical velocity difficult. Similarly, Chino and Ishikawa [2] observe that the mass-consistency of the used wind field is essential for avoiding unrealistic source/sink effects in the calculation of transport and diffusion processes. Numerical models can solve all these problems.

Models simulating wind flows over rough terrain can be divided into two types: "prognostic", "predictive", "dynamic" or "primitive equation" models and "diagnostic" or "kinematic" models. Prognostic models are based on the solution of timedependent hydrodynamic and thermodynamic equations (called primitive equations as they are derived straight from the original conservation principles), appropriately modified to apply into the atmosphere. These models are also called dynamic (for instance by [3]) to indicate the explicit inclusion of the dynamic equations. Models of this nature generally include the effects of advection, stratification, Coriolis force, radiation and turbulent fluxes of momentum, heat and moisture. The solution of the full set of equations, however, still remains a laborious and expensive task. Furthermore, the more elaborate the model, the more reliable the input data should be in order to exploit the advantages offered by the model: often these data are not available. Furthermore, due to their complexity and cost, these models are generally run for a few cases only, usually corresponding to the most significant meteorological events that affect the considered

Lalas [3] includes among dynamic codes a few models which introduce strong approximations into the primitive equations, while neglecting their time-dependence. These codes, we call JH models, are based on a Jackson and Hunt [4] proposal.

Diagnostic codes merit this name since, as observed by Pielke [5], they are not used to forecast forward in-time through the integration of the conservation relationships. For this same reason, they are also called (again by [3]) kinematic models. These models generate a wind field by satisfying some physical constraints. If, for example, only the continuity equation

^{*}This study has been supported by the CNR-ENEL project "Interactions of energy systems with human health and environment", Rome, Italy.

[†]Pe. manent address: Centro Nacional Patagonico, Puerto Madryn, Chubut, Argentina.

- which assures mass conservation - is imposed, the wind model is defined mass-consistent. These models are based on the numerical solution of the steady state three-dimensional continuity equation for the mean wind components. The momentum and energy equations are, as observed by Dinar [6], not solved explicitly but considered indirectly using parametric relations and/or wind data.

The relative simplicity of diagnostic wind models makes them attractive for many practical purposes, in that they do not require much input data and are easy and economical to operate. In fact, these models quickly and efficiently utilize available data to generate a wind field which satisfies some physical constraints.

Furthermore, Pennel [7] found that in some cases the "improved mass-consistent models" outperformed the more complicated and expensive dynamic models. Similarly, Burch and Ravenscroft [8] claim that these simple models work considerably better than the others in normal situations where crucial data needed to run the more sophisticated models are not available.

On the other hand, diagnostic (both JH and mass-consistent) models do not take into account thermal effects and effects due to changing pressure gradients. As a consequence, flows such as sea breezes, slope winds, heat island effects, etc. as well as downwind separation effects cannot be simulated, unless embedded in the initial wind data from observations at the appropriate location: see for example [9] for separation effects and [1, 10, 11] for land/sea breeze. Diagnostic models are thus specifically designed to predict the effects of orography on steady mean wind flows (i.e. flows averaged over time intervals that vary between 10 min and 1 hour).

According to Troen [12], the JH approach has to be preferred to the mass-consistent method, due to the fact that it uses more physical constraints than just the continuity equation. On the other hand, the mass-consistent models do have the advantage of easily taking into consideration observed values of the wind field at several different points and/or distances from the ground, while JH models usually, but not necessarily, describe the modifications of an "unperturbed flow" produced by the orography under consideration. Furthermore, steep slopes affect JH models more critically than mass-consistent models.

The aim of this work is to highlight the fundamental aspects of, and differences between, mass-consistent models developed over the last fifteen years.

Kitada et al. [1] have classified objective analysis of wind field data into four types of models, all of which use the continuity equation as the constraint equation, while differing in the manner in which this result is obtained. In this paper we only examine the methods belonging to Kitada's "variational calculus method"

class.

Our analysis is essentially based on the following models: MASCON [13], MATHEW [14], NOABL [15-17], COMPLEX [18-20], WINDO4 [21, 2], ATMOS1 [22], BOLOS³ [23, 26], REDBL and CONDOR [10, 11, 27], MINERVE [28], NUATMOS [29-31], MC-3 [32], WINDS [33] and LSWIND [34]. For the meaning of the acronyms, see Appendix A.

1. THE GENERAL APPROACH

1.1. The inizialization and the adjustment steps

Mass-consistent models describe the wind flow over terrain with complex orography. Following Moussafir [35], we call the domain of application of the model Ω and assume we know the value of the wind vector (intensity and direction) in N points of Ω : $\vec{V}_1, \vec{V}_2, \ldots, \vec{V}_N$. The aim is to construct a flow field over the entire domain which assumes the known values at the considered points, while at the same time satisfying the continuity equation. The solutions possible are infinite. In order to obtain the final solution two steps are required

i) An initialisation step \aleph which transforms, through interpolation/extrapolation, the N given wind vectors in a wind field over all Ω , according to the following schema

$$(\vec{V}_1, \vec{V}_2,, \vec{V}_N) \stackrel{\aleph}{\rightarrow} \vec{V}^o(z, y, z)$$
.

The \vec{V}^o field is called "initial", "first guess", "initial guess" or "observed" field and does not normally satisfy the continuity equation.

ii) An adjustment step or minimisation procedure \Im which minimally adjusts the \vec{V}^o field to construct the "adjusted", "final" or "reconstructed" field \vec{V} that satisfies the mass conservation according to the following scheme

$$\vec{V}^o(x,y,z) \stackrel{\Im}{\to} \vec{V}(x,y,z)$$
.

It should be emphasised that the final solution depends both on the adopted \aleph and \Im . The \Im process is nearly the same for almost all the models considered (see section 2), although the numerical solutions of the governing equations can differ (see section 6). The \aleph process varies substantially from one code to another (see section 5).

A comparison between the output of a mass—consistent model and one or more reference sites (obviously not included in the input data set) generally shows that there may be a poor agreement with measurements at single points. Agreement, however, is much better if the average wind over the region is considered.

³Called NOABL* in [23] and [24] and AIOLOS in [25].

In other words, the model cannot provide wind values close to the measured data at every point, but does give satisfactory values for the general flow over the region. This is not surprising, since many of the physical processes affecting the flow over terrain are not simulated in mass—consistent models. For a further discussion relating to these problems see sections 5.1 and 5.2.

1.2. Continuity equation

The continuity equation in its general form is

$$\frac{\partial \rho}{\partial t} + \vec{\nabla} \cdot (\rho \vec{V}) = 0 \quad . \tag{1}$$

If we assume that the air density is constant, equation (1) becomes

$$\vec{\nabla} \cdot \vec{V} = 0 \quad . \tag{2}$$

This equation is used by most of the models and is called the "uncompressible form of the continuity equation", distinguishing it from the "anelastic form"

$$\vec{\nabla} \cdot (\rho \vec{V}) = 0 \tag{3}$$

considered by Mathur and Peters in [36]. Equation (3) has the advantage of taking into account variations in density. These variations can occur, for example, if very large domains are considered, or if there are large heat sources or sinks in the domain — such as lakes, towns or valleys non-uniformly exposed to the sun—that can induce strong differences in temperature even between relatively close regions.

To determine the effect of the variable density on the model output, Endlich et al. [19] ran their model either with constant or with variable density, decreasing with height according to standard atmospheric values, all other conditions in the run being identical. They found that the differences in the results were barely detectable.

Dickerson [13], in the two-dimensional model MASCON, utilises a direct consequence of the mass conservation law, which is

$$\frac{\partial z_{bi}}{\partial t} + \frac{\partial (uz_{bi})}{\partial x} + \frac{\partial (vz_{bi})}{\partial y} + w = 0$$

where z_{bl} is the height of the inversion base above orography, assumed variable in time; u and v are the components of the wind vector in the x and y directions, averaged within the sub-inversion layer (see section 5.3.1), and w is the vertical outflow velocity through the inversion base.

2. THE VARIATIONAL TECHNIQUE

2.1. Sasaki's method

All the models examined in this paper use Sasaki's method [37, 38] to obtain the adjusted field. The adjustment procedure of the wind field \vec{V}^o , defined in section 1.1, can be performed using variational calculus. The general variational analysis formalism defines an integral function, the extremal solution of which minimizes the variance of the difference between the observed and the adjusted variable values subject to physical constraints which have to be satisfied, exactly or approximately, by the adjusted values. It should be remembered that the subsidiary conditions to be satisfied exactly are k town as "strong constraints", while conditions imposed approximately are called "weak constraints". A "minimal solution" exists when the number of strong constraints is less than the number of variables.

To obtain such a solution, mass-consistent models minimize the variance of the difference between the adjusted values and the observed values

$$E(u, v, w) = \int_{\Omega} \left[\alpha_1^2 (u - u^o)^2 + \alpha_2^2 (v - v^o)^2 + \alpha_3^2 (w - w^o)^2 \right] dV$$
 (4)

under the strong constraint of mass conservation. In this equation (u^o, v^o, w^o) and (u, v, w) are the components of $\vec{V}^o \in \vec{V}$ respectively, and Ω is the domain defined in section 1.1.

Note that since measurements of the vertical velocity component are seldom available, the initial vertical velocity w^o is usually set to zero at each grid point. Barnard et al. [39, 40] set w^o equal to zero at all grid points, except at the lower boundary where w^o is calculated so that the initial wind is parallel to the terrain surface (see also section 2.2).

The problem of minimizing the expression of equation (4) under the strong constraint (2) is equivalent to minimizing the following functional

$$J(u, v, w; \lambda) = \int_{\Omega} \left[\alpha_1^2 (u - u^o)^2 + \alpha_2^2 (v - v^o)^2 + \alpha_3^2 (w - w^o)^2 + \lambda \left(\frac{\partial u}{\partial x} + \frac{\partial v}{\partial y} + \frac{\partial w}{\partial z} \right) \right] dV$$
(5)

where $\lambda = \lambda(x, y, z)$ is the Lagrange multiplier (which represents, physically speaking, the perturbation velocity potential) and the values of α_i (i = 1, 2, 3) are the Gauss precision moduli.

Identical Gauss precision moduli are always assumed for the horisontal directions⁴, while distinctions be-

⁴ For this reason both α_1 and α_2 are usually called α_1 , while our α_3 appears as α_2 .

tween horisontal and vertical directions are apparent (see section 3).

Dickerson [13], Sherman [14] and Mathur and Peters [36] assume that

$$\alpha_i^2 = \frac{1}{2\sigma_i^2}$$

where the values of σ_i represent the variances relative to the observation errors and/or the deviations of the observed field from the adjusted field. For the consequences of this assumption refer to section 3.

The Euler-Lagrange equations, the solution of which minimizes equation (5), are

$$u = u^{o} + \frac{1}{2\alpha_{1}^{2}} \frac{\partial \lambda}{\partial z}$$

$$v = v^{o} + \frac{1}{2\alpha_{2}^{2}} \frac{\partial \lambda}{\partial y}$$

$$w = w^{o} + \frac{1}{2\alpha_{3}^{2}} \frac{\partial \lambda}{\partial z}$$
(6)

Note that Bhumralkar et al. [18], Endlich et al. [19] and Endlich [20] use the notations $\alpha_1^2 = \alpha_2^2 = W_H$ and $\alpha_3^2 = W_V$; Guo and Palutikof [32] set $1/(2\alpha_1^2) = 1/(2\alpha_2^2) = \tau_h$ and $1/(2\alpha_3^2) = \tau_v$ and call τ_h (τ_v) "horisontal (vertical) transmissivity", while Troen [41] simply calls $(\alpha_1/\alpha_3)^2 = \tau_v/\tau_h = \tau$ "transmissivity".

In the COMPLEX approach [18-20] λ is eliminated from equations (6) obtaining three uncoupled equations for the wind components

$$\frac{\partial^{2} u}{\partial x^{2}} + \frac{\partial^{2} u}{\partial y^{2}} + \left(\frac{\alpha_{1}}{\alpha_{3}}\right)^{2} \frac{\partial^{2} u}{\partial z^{2}} \\
= \frac{\partial^{2} u^{o}}{\partial y^{2}} + \left(\frac{\alpha_{1}}{\alpha_{3}}\right)^{2} \frac{\partial^{2} u^{o}}{\partial z^{2}} \\
- \frac{\partial}{\partial x} \left(\frac{\partial v^{o}}{\partial y} + \frac{\partial w^{o}}{\partial z}\right) \\
\frac{\partial^{2} v}{\partial x^{2}} + \frac{\partial^{2} v}{\partial y^{2}} + \left(\frac{\alpha_{1}}{\alpha_{3}}\right)^{2} \frac{\partial^{2} v}{\partial z^{2}} \\
= \frac{\partial^{2} v^{o}}{\partial x^{2}} + \left(\frac{\alpha_{1}}{\alpha_{3}}\right)^{2} \frac{\partial^{2} v^{o}}{\partial z^{2}} \\
- \frac{\partial}{\partial y} \left(\frac{\partial u^{o}}{\partial x} + \frac{\partial w^{o}}{\partial z}\right) \\
\frac{\partial^{2} w}{\partial x^{2}} + \frac{\partial^{2} w}{\partial y^{2}} + \left(\frac{\alpha_{1}}{\alpha_{3}}\right)^{2} \frac{\partial^{2} w}{\partial z^{2}} \\
= \frac{\partial^{2} w^{o}}{\partial x^{2}} + \frac{\partial^{2} w^{o}}{\partial y^{2}} \\
- \left(\frac{\alpha_{1}}{\alpha_{3}}\right)^{2} \frac{\partial}{\partial z} \left(\frac{\partial^{2} u^{o}}{\partial x} + \frac{\partial^{2} v^{o}}{\partial y}\right) .$$
(7)

Assuming that $\alpha_1 = \alpha_2$ and α_3 are constant throughout the domain, all other models using the variational

approach derive the elliptic equation for λ

$$\frac{\partial^{2} \lambda}{\partial x^{2}} + \frac{\partial^{2} \lambda}{\partial y^{2}} + \left(\frac{\alpha_{1}}{\alpha_{3}}\right)^{2} \frac{\partial^{2} \lambda}{\partial z^{2}}$$

$$= -2\alpha_{1}^{2} \left(\frac{\partial u^{o}}{\partial x} + \frac{\partial v^{o}}{\partial y} + \frac{\partial w^{o}}{\partial z}\right)$$
(8)

by differentiating equations (6) and substituting the results into continuity equation (2).

Ross et al. [29] explicitly pointed out that if the right hand side of this equation vanishes (for instance, if \vec{V}^o represents a uniform background wind) and if $\alpha_1 = \alpha_2 = \alpha_3$, then λ represents a velocity potential. Thus the resulting solution to the problem, subject to nonnormal flow through the terrain boundary, will be the potential flow.

Mathur and Peters [36] impose a second strong constraint which represents the conservation of the z component of vorticity

$$\zeta = \frac{\partial v}{\partial x} - \frac{\partial u}{\partial y}$$

in the transformation from the \vec{V}^o to the \vec{V} field. This constraint emerges from the fact that these authors want the adjusted field to maintain the most important physical properties of the observed field (and vorticity is one of them). Since vertical components of the wind velocity are not routinely measured, Mathur and Peters claim that it is desired to preserve the vertical component of vorticity. With the above approach, the functional (5) contains an additional term and thus becomes

$$J(u, v, w) = \int_{\Omega} \left[\alpha_1^2 (u - u^o)^2 + \alpha_2^2 (v - v^o)^2 + \alpha_3^2 (w - w^o)^2 + \lambda_1 \left(\frac{\partial u}{\partial x} + \frac{\partial v}{\partial y} + \frac{\partial w}{\partial z} \right) + \lambda_2 \left(\frac{\partial v}{\partial x} - \frac{\partial u}{\partial y} \right) \right] dV$$

with the corresponding Euler-Lagrange equations becoming

$$u = u^{o} + \frac{1}{2\alpha_{1}^{2}} \frac{\partial \lambda_{1}}{\partial x} + \frac{1}{2\alpha_{1}^{2}} \frac{\partial \lambda_{2}}{\partial y}$$

$$v = v^{o} + \frac{1}{2\alpha_{2}^{2}} \frac{\partial \lambda_{1}}{\partial y} + \frac{1}{2\alpha_{2}^{2}} \frac{\partial \lambda_{2}}{\partial x}$$

$$w = w^{o} + \frac{1}{2\alpha_{2}^{2}} \frac{\partial \lambda_{1}}{\partial z}$$

On the other hand, Ross and Smith [42] correctly point out that it can be easily shown from equations (6) that, on the assumption that $\alpha_1 = \alpha_2$ and α_3 are independent of z and y and that λ is well-behaved, the vertical component of vorticity is automatically conserved.

Thus, the inclusion of this additional constraint is unnecessary and adds a considerable computation burden. Furthermore, note that, if $\alpha_1 = \alpha_2 = \alpha_3$ is independent of x, y and z and λ is well-behaved, the three components of vorticity are conserved.

2.2. Boundary conditions

From the development of the variational problem, the following boundary conditions can be obtained

$$\lambda \delta \vec{V} \cdot \vec{n} = 0 \quad \text{on} \quad \Gamma \tag{9}$$

where Γ is the surface of the domain. Here the notation $\delta \vec{V}$ denotes the first variations of the velocity and \vec{n} is the outward unit vector normal to the surface of the domain.

As either λ or the normal velocity component variation must be zero at a boundary, and as we cannot impose both of them (the solution would no longer be unique), the following choice is adopted by Sherman [14] and almost all other authors

- $\lambda=0$ or "natural boundary conditions" for open or "flow-through" boundaries. This condition implies that the normal derivative of λ is, in general, different from zero. Thus, a non-zero adjustment of the observed velocity component normal to the boundary may occur. As results from equations (6), a change in the amount of mass entering or leaving the volume can occur.
- $\frac{\partial \lambda}{\partial n} = 0$ i.e. Neumann boundary conditions, for closed or "no-flow-through" boundaries. Again from equations (6), this implies, at least with Cartesian coordinates (see section 4.2), that there is no adjustment in the normal velocity component, i.e. $\delta \vec{V} \cdot \vec{n} = 0$. If the observed normal velocity component through the boundary is zero, the adjusted flow of mass across the boundary is also zero, and the condition is then appropriate for closed boundaries, as are the terrain and possibly the top of the domain when assumed to be an inversion base.

Models using conformal coordinates (see section 4.3) replace the last condition with $\vec{V} \cdot \vec{n} = 0$ at the solid boundaries.

Barnard et al. [39, 40] and Ross et al. [29] explicitely pointed out that the closed boundary condition has to be used along with the requirement that the initial surface flow is parallel to the surface in order to satisfy the impenetrability constraint.

Sherman [14] noted, even though not using this possibility, that the Neumann boundary condition can also be used to specify known transport of mass across an open boundary. Ishikawa [21] investigated both boundary conditions for open boundaries, simulating

a two-dimensional triangular hill, and found that imposing a sero adjustment of the normal velocity component over all the boundary gives a better agreement with observations. The principal effect of this choice is that the ill boundary effects present in such simulations completely disappear.

This same approach was used by Ishikawa [34] in his simulation of the Chernobyl incident and by Takeuchi and Adachi [43] in their study of the Kansai area, Japan. Nevertheless, it has to be remembered that, when imposing Neumann boundary conditions to all boundaries with an elliptic equation, singularity problems can arise as soon as the first guess does not have zero mass flow through the boundaries of the simulated volume.

3. PARAMETRIZATION OF STABILITY

All the simulations performed with mass-consistent models showed that these codes are very sensitive to the values chosen for $\alpha_1 = \alpha_2$ and α_3 in the equations of section 2.1. Therefore, particular attention must be given to this problem. Barnard et al. [39, 40] point out that the difficulty in determining the correct values to give to these parameters has limited the possible wide use of mass-consistent models for quantitative predictions of windiness in complex terrain.

As the functional (5) has to be minimised, dividing it by a constant value, i.e. α_3^2 , makes no difference except for numerical effects. A unique parameter is thus introduced

$$\alpha^2 = \frac{\alpha_1^2}{\alpha_3^2} = \frac{\tau_v}{\tau_h} = \tau$$

where τ_0 , τ_h and τ are the transmissivities defined in section 2.1. Barnard *et al.* [39, 40] prefer to consider the logarithm of this quantity

$$\tau = \log \frac{\alpha_1^2}{\alpha_3^2} = 2\log \alpha .$$

This parameter τ is called the "empirical stability parameter".

Note that the coefficients $\alpha_1^2 = \alpha_2^2$ and α_3^2 are the weights of the horisontal and vertical adjustments of the velocity components. Thus, for $\alpha >> 1$, flow adjustment in the vertical direction predominates, so that air is more likely to go over a terrain barrier rather than around it, while for $\alpha << 1$, flow adjustment occurs primarily in the horisontal plane, so that air is more likely to go around a terrain barrier rather than over it. In particular, $\alpha \to \infty$ signifies pure vertical adjustments, while $\alpha \to 0$ signifies pure horisontal adjustments.

Sherman [14], followed by Kitada et al. [1], by Mathur and Peters [36] and by Davis [22], suggested that the

value of α , being equal to σ_3/σ_1 (see section 2.1) should be proportional to the magnitude of the expected w/u, and thus should be taken as equal to 10^{-2} if one wants to correctly weigh horizontal and vertical adjustments.

Kitada et al. [1] simulated a two-dimensional land/sea breeze circulation with strong vertical motions. They evaluated $w/u \simeq 0.22 \div 0.50$ and thus made simulations with $\alpha \simeq 0.10$ and 0.32, finding that the larger value gives a slightly preferable wind flow.

The same authors, in their simulation of the three-dimensional wind flow in the Mikawa Bay area, allowed α to vary from 0.01 to 0.22, finding a minimum total divergence at $\alpha=0.10$. On the other mand, smaller values of α increasingly smoothed out, in the adjusted wind field, the substantial irregularities shown by the initial wind field.

As a conclusion, Kitada et al. observed that data available on the magnitude of w/u are very helpful for establishing an appropriate value of α . The best value of α should be determined by considering the total residual divergence, the flow pattern and the expected value of w/u.

Davis [22] suggests that $\alpha \sim 0.01$ is suitable for a stable atmosphere, while under unstable conditions α would tend toward infinity.

Endlich et al. [19] state that, in their simulations, values of $W_H/W_H = (\alpha_1/\alpha_3)^2$ in the range 10^{-10} to 10^{-12} give suitable results. On the other hand, as explained by Endlich [19], stability effects are produced, in this approach, by changing the height of the computational domain (see section 4.4).

Guo and Palutikof [32], in their validation of NOABL, used α values equal to 1.0 for neutral conditions, down to 0.1 for a very stable atmosphere and up to 5.0 for very unstable conditions. In predicting high wind speeds ⁵, they found a less than 8% wind speed change as the α value moved from 1.0 to 0.1, and a less than 2% wind speed change as the α value moved from 1.0 to 5.0.

Ishikawa [34] — in the development of the WSPEEDI — found the values of α in the range 0.005 to 0.010 suitable in the model LSWIND, when used for simulating synoptic wind fields (see section 4.7).

Barnard et al. [39, 40], in their tuning of the NOABL model through the use of an optimisation technique, which will be discussed in section 7, found values of $\tau = 2\log\alpha$ between -0.98 to 0.06, corresponding to α between 0.62 to 1.03, excluding cases where winds were light to moderate (in these cases τ could be as small as -1.65, corresponding to $\alpha \sim 0.44$).

Barnard et al. proposed a procedure for accurately de-

termining the stability parameter for each individual models application. If several observed wind speeds are available, some are not used to calculate the wind field but are kept as a reference. Several simulations are then performed using the remaining observations and different values of α . The final value is the one that gives the best agreement with the reference observations. It should be noted that this method provides values of α that are only reliable for the particular case under analysis. As a consequence, this method cannot provide an a priori value that can be used for other simulations, but must be applied entirely to each simulation.

Some authors make the α coefficient vary in the domain. Lalaz [23, 26] applied this idea introducing a transmissivity coefficient variable in the vertical direction. The MINERVE code [28] allows the use of a vertical profile or of a 3D distribution of α .

Other authors claim that α should depend not only on stability, but also on the characteristics of orography. Some authors (such as Troen [41], Ross et al. [29], Moussiopoulos et al. [11, 27] and Georgieva [44]) have attempted to relate α to the Froude number, which is defined as

$$Fr = \frac{U}{N\mathcal{H}}$$

where U is the velocity scale or the characteristic wind speed, \mathcal{H} is the characteristic height difference and \mathcal{N} is the buoyancy frequency or Brunt-Väisälä frequency

$$\mathcal{N} = \sqrt{\frac{g}{\theta}} \frac{d\theta}{dz}$$

 θ being the potential temperature. A simple physical interpretation of the Froude number is the ratio between the kinetic and the buoyant energy of an air parcel. The Froude number is considered as a suitable parameter since it depends both on stability, through the buoyancy frequency, and on orography, through the height difference.

Troen [41] has developed a mass-consistent model based on the Fourier transform of equation (8) in which the transmissivity τ is treated as wavenumber dependent. This author assumes that near the surface

$$au_{k,l} = 1 + (au_{k,l}^l - 1) \exp[-0.3z_{\mathrm{M}}(k^2 + l^2)^{1/2}]$$

where k and l are the wavenumbers in the x and y directions, z_{kl} is the Planetary Boundary Layer (PBL, in the following) height and $\tau'_{k,l}$ is the transmissivity above the PBL. It is assumed that

$$au'_{k,l} = Fr^2 = rac{u_G k + v_G l}{N} ext{ if } Fr \leq 1$$
 $au'_{k,l} = 1 ext{ if } Fr > 1$

where u_G , v_G are the components of the velocity above the PBL.

⁵The wind was predicted on a site from the data recorded in a station 4.6 kilometres away and with an elevation 250 metres less.

Ross and Smith [29] found that, for neutral and stable flows over a hill, it is more suitable to use the function

$$\alpha^2 = 1 - \frac{\alpha}{\sqrt{Fr}}$$
 if $z > H_c$

 $\alpha^2 = 0$ if $z \le H_c$

where $a \simeq 0.7$ and H_c is the upstream height of the streamline dividing the air flowing above the hill from the air flowing round it. The determination of the value of H_c is quite difficult; for stable and neutral flows, Hunt and Snyder [45] propose

$$H_c \geq h(1 - Fr)$$

where h is the height of the hill.

Subsequently, Ross [30, 42], having used additional laboratory data, suggested the relationship

$$\alpha^2 = 1 + \frac{3}{(S^2 - 1)Fr^2} \tag{10}$$

where S is the "speedup" over the terrain. In 1993, the same research group (see [31]) claimed that further testing using field data for complex terrain is needed before expression (10) can be routinely used within an operational version of NUATMOS.

Moussiopoulos et al. [11, 27] partially followed the Ross and Smith approach, preferring to use the inverse of the Froude number, the Strouhal number which, in neutral and stable conditions $(d\theta/dz \ge 0)$, is defined

$$Str = \frac{\mathcal{NH}}{U}$$

where N is the already defined buoyancy frequency, and, in unstable conditions $(d\theta/dz < 0)$, is defined as

$$Str = -\frac{\mathcal{H}}{Ut}$$

where t is the buoyancy time scale

$$\frac{1}{t} = \sqrt{-\frac{g}{\theta} \frac{d\theta}{dz}} .$$

After a comparison of the numerical results with experimental data, Moussiopoulos et al. suggested that a good parametrisation for α in stable flows should be

$$\alpha^2 = 1 - \frac{Str^4}{2} \left(\sqrt{1 + 4Str^{-4}} - 1 \right)$$

if $Str \geq 0$.

If Str < 0 the relationship

$$1<\alpha^2<\left[\alpha^2(-Str)\right]^{-1}$$

is proposed. Nevertheless, Moussiopoulos et al. observe that the parametrization for unstable stratification has no significant influence on the resulting wind field.

These relationships give α varying between 1 and 0 with Str passing from 0 to 3, and α rising from 1 to ~ 2.6 with Str passing from 0 to -1.

The value of Str and thus of α is calculated [11, 27] at every grid point through the following procedure

i) the characteristic height difference H

$$\mathcal{H}_{kl} = \frac{\sum_{i,j\neq k,l} |\Delta h_{ij}|/r_{ij}^2}{\sum_{i,j\neq k,l} 1/r_{ij}^2}$$

where Δh_{ij} and r_{ij} are the orographic height difference and the horizontal distance respectively between points (i, j) and (k, l). Note that this equation gives high values of \mathcal{H} at locations close to steep slopes of the terrain;

- ii) the Brunt-Väisälä frequency \mathcal{N} or the buoyancy time scale t are deduced from vertical temperature profiles from upper air soundings;
- iii) the characteristic wind speed U is set equal either to $0.2 \, m/s$ or to the local first-guess wind velocity, provided that this exceeds $0.2 \, m/s$;
- iv) for convergence reasons, the local values of $\alpha_{i,j,k}$ are usually not allowed to be less than $1/\sqrt{30}$ and greater than $\sqrt{30}$.

4. DISCRETIZATION OF THE DOMAIN

4.1. The 3-D grid

For the application of any mass-consistent model it is necessary to discretize the Ω region by introducing a three-dimensional grid.

First of all, the terrain elevation for each node of a horizontal rectangular grid, usually with square cells, has to be specified. This elevation can represent an average value relative to the cell containing the node or the elevation of the grid point.

Two of the wind models considered here, EOLOS [23, 26] and WINDS [33], also need a discretisation of the terrain roughness relative to the same grid points used for the orography.

In mass-consistent wind models, two kinds of discretization of the volume above ground are used: Cartesian and conformal coordinates.

4.2. The Cartesian coordinate system

The Cartesian system of coordinates is used in the MASCON [13], MATHEW [14] and LSWIND [34] models and can be used optionally in NOABL [15-17]. Furthermore, the Cartesian coordinates are used in models simulating flow between buildings, as in [46].

In this case, the computational domain consists of a rectangular box, with the bottom of the box located at the lowest topographic point in the area. Within the computational domain, the volume is subdivided into rectangular cells with dimensions Δx , Δy , Δz in the x, y, z directions respectively. Usually $\Delta x = \Delta y$. The orography is represented by "obstacle cells". An obstacle cell is defined as a computational cell whose faces are treated as impermeable boundaries. Obstacle cells are created whenever the terrain surface passes above or through the upper half of a computational cell.

It should be noted that the degree to which the terrain surface is represented by obstacle cells is strongly dependent on the chosen cell resolution. This can be a drawback to the efficient computation of windfields over complex terrain. Furthermore, the coordinate system makes boundary conditions near the ground difficult to satisfy. As a consequence, as Lowellen et al. [47] showed, this surface representation leads to large velocity errors near the surface.

4.3. Terrain conformal coordinate system

For regions in which the terrain varies substantially, it is advisable to choose "terrain conformal" coordinates, also called "conformal", "terrain-following" or "sigma" coordinates by many authors. In this case, the orography determines the coordinate mesh. The use of the conformal transformation has several advantages:

- i) the terrain surface is more accurately represented, due to the characteristics of the transformation itself;
- ii) conformal coordinates also imply simpler boundary conditions (see the end of this section); and
- iii) conformal coordinates make the use of variable vertical soning easier, allowing higher resolution near the terrain surface without penalising efficiency.

Finardi et al. [9], in their testing of MATHEW and MIN-ERVE, underline the effectiveness of terrain-following coordinates compared to the Cartesian ones.

The coordinate transformation is

$$\xi = x$$

$$\eta = y$$

$$\sigma(x, y) = \frac{z - h(x, y)}{H(x, y) - h(x, y)}$$
(11)

where h(x, y) is the height of the terrain above a reference level (not necessarily sea level), and H(x, y) is the corresponding height of the top of the domain, which is usually assumed to be rigid and impermeable. H is often assumed equal to the height z_{bl} of the elevated temperature inversion base, the presence of which prevents the outflow of air: for more details see section 4.4. The transformation (11) is purely geometric. It is evident from definition (11) that σ is constant both

at the bottom $(\sigma = 0)$ and at the top $(\sigma = 1)$ of the domain.

The MINERVE code [28] uses $s = \sigma H$ instead of σ , with H assumed constant. The codes NOABL [15-17], ATMOS1 [22], EOLOS [23, 26], NUATMOS [29-31], REDBL and the first version of CONDOR [10] and WINDS [33] use, instead of σ , the quantity σ'

$$\sigma' = 1 - \sigma \tag{12}$$

so that $\sigma' = 0$ at the top of the domain and $\sigma' = 1$ at the terrain surface. The CONDOR code [11] uses $s = \sigma' H$.

The components of the velocities $(\tilde{u}, \tilde{v}, \dot{\sigma})$ in the terrain-following coordinates are easily obtained by differentiating expressions (11) or (12) with respect to time

Note that the "no-flow-through" condition at the terrain surface and at the top of the domain (see section 2.2) simply becomes, in conformal coordinates, $\dot{\sigma} = 0$ or $\dot{\sigma}' = 0$.

Kitada et al. [1, 48], Bhumralkar e. al. [18] and Endlich et al. [19] introduce the variables $u^* = \Delta H \bar{u}$, $v^* = \Delta H \bar{v}$ and $w^* = \Delta H \dot{\sigma}$, where $\Delta H = H - h$. This allows expressions in conformal coordinates to be obtained equal to those given by equations (2), (5), (6), (7) and (8), provided that coordinates x, y and z are replaced by ξ , η and σ respectively and speeds u, v and w are replaced by quantities u^* , v^* and w^* respectively. This result is obtained by minimising the functional (5) written in conformal coordinates with respect to the new variables u^* , v^* and w^* . Ross et al. [29] claim that this approach does not readily lead to the correct flow in the simple test cases examined by them.

While Kitada et al. work with equations (6) and (8) rewritten as just stated, in the COMPLEX model [18, 19], equation (7), with x replaced by ξ and u replaced by u^* and so on, is used: for more information about this approach, see section 6.

The other authors working with conformal coordinates transform equations (2), (5), (6) and (8) in conformal coordinates. In other words, they minimise functional (5) with respect to variables u, v and w and not with respect to \tilde{u} , \tilde{v} and $\dot{\sigma}$.

4.4. Height of the domain

Most of the mass-consistent models assume H = const in equation (11). With this choice, the conformal surfaces are terrain-following near the terrain itself, while becoming flatter with increasing z.

Kitada et al. [1, 48] assume, in equation (11), $H-h \simeq 1000 \, m$ constant in all the domain. With this choice the conformal surfaces are terrain-following at all elevations.

Endlich et al. [19, 20] assume

$$H(x,y) = H_a + kh(x,y) + (1-k)h_k$$
 (13)

where h, is the terrain height at a site of interest, H_a is the average thickness of the PBL at the same site and k is a "slope factor". If k = 0 the top of the boundary layer is flat, if k = 1 the top is parallel to the terrain. Values greater than 1 give slopes steeper than the terrain slope; negative values give slopes opposite to the terrain slope. The parameters H_a and k can be treated as functions of time of day and season. Endlich suggests that their typical values are $H_a = 500 m$ and k = 0.2, for the nighttime case, and $H_a = 1500 m$ and k = 0.8 for the daytime case. Endlich et al. [19] point ou that they assume a sudden transition in the depth of the boundary layer from daytime to nighttime values, and vice versa, which is only an approximation to reality. Furthermore, these authors observe that equation (13) can give unrealistically low values of the PBL top over the highest terrain unless an iterative procedure is adopted, compelling the minimum PBL thickness to be greater than 200 m.

Guo and Palutikof [32] suggested selecting the PBL height with the following procedure. First they select a station as the "tuning station" for the area. Then the PBL height is decided by comparing predicted and observed wind speeds at the tuning station for different PBL heights. The PBL height which gives the best prediction is selected (see also section 7).

The top of the domain must always be above the highest terrain. In fact, Sherman [14] observed that the orography may protrude through the top of the grid, potentially producing unconnected regions within the grid volume, but we could not find any such application in the literature on these models.

On the other hand, Moussafir [49] suggests that $H - h_{min}$ should, in any case, be greater than twice the maximum orographic height difference, i.e.

$$H-h_{min}>2(h_{max}-h_{min})$$

 h_{max} and h_{min} being the highest and the lowest grid point levels respectively.

4.5. Horisontal spacing

In almost all the models using Cartesian coordinates, a constant grid spacing is used for both the horisontal directions.

Bhumralkar et al. [18], Endlich et al. [19] and Tombru and Lalas [26] optimise the (accuracy/computational time) ratio with a procedure that uses the output of the simulation carried out with a coarse grid as an input for a new simulation carried out with a finer grid, defining orography and possibly roughness with greater detail. The new grid is chosen in such a way that all the nodes of the coarse grid remain nodes of the

fine grid; the input value is thus known for all these nedes. For the other nodes, the input wind value is obtained through interpolation of the coarse grid wind values.

Tombru and Lalas point out that this procedure can be repeated with an even finer grid until the required accuracy is reached. An effect of this iteration is that the code "sooms" into the area of interest; thus the method is called a "telescoping procedure" by its authors.

The relatively small increase in computational effort, compared to the appreciable results that have been obtained [26], shows that this approach is a good solution if simulations in zones with complex orography are requested.

4.6. Vertical spacing

The models that use Cartesian coordinates usually impose $\Delta z = const.$ Only Takeuchi and Adachi [43] use vertically stretched coordinates with higher resolutions at low levels. On the contrary, as we have already stated, variable vertical zoning is common with terrain conformal coordinates.

If a discretisation in σ given by equation (11) is performed in order to have N levels (including $\sigma=0$ and $\sigma=1$), the distance between two consecutive levels in real space is

$$\Delta z_k(x,y) = [H(x,y) - h(x,y)] \Delta \sigma_k \tag{14}$$

subjected to the condition

$$\sum_{k=1}^{N-1} \Delta z_k = H(x, y) - h(x, y) .$$
 (15)

A more general transformation between z and σ is used in the MC-3 model [32] which assumes, as does COMPLEX [20], no flow through the terrain-following coordinates (see also considerations on this topic in section 6). This transformation produces the following spacing

$$\Delta z_k(x,y) = \left[H_a + C\left(1 - \frac{k}{N}\right)^q \right] \times \left(H(x,y) - h(x,y) - H_a\right] \Delta \sigma_k$$
(16)

where H_a is the PBL thickness over the test region and C is determined from equation (15).

The parameter q, which is positive and smaller than 1, is assumed to be linked to the atmospheric stratification. Note that if q=0 then C=1 due to equation (15): thus equation (16) becomes the same as equation (14). As the value of q increases from 0 to 1, near surface wind flow tends to be restricted to a smaller (greater) vertical height above high (low) ground. The value for q can be chosen in order to obtain the best agreement with the observations.

As k increases, the difference between $\Delta z_k(x, y)$ and $H_a \Delta \sigma_k$, i.e. the average layer thickness for that particular layer, decreases. When k reaches the value of N, this difference is reduced to nothing, i.e. $\Delta z_k = const$. Once the algorithm converting z into σ has been defined, the problem of choosing the spacing in this new space still exists. The simplest choice consists of the constant vertical spacing option used by references [1, 48], i.e. $\Delta \sigma_k = const$.

To improve the resolution near the terrain, in order to increase the density of the levels where the wind velocity vertical gradient is higher, most models allow the user to select a grid with variable spacings. Four kinds of such spacing are commonly used

i) log-linear distribution, as used in ATMOS1; this spacing is generated by the following equation

$$\sigma_k = \sigma_{k-1} + 0.2 \,\sigma_{k-1} \log \left(c + \sigma_{k-1}\right) \tag{17}$$

where $c \simeq 0.001$ prevents the argument of the logarithm from becoming zero;

ii) geometric distribution, which can be used as an option in NOABL, BOLOS and WINDS together with the log-linear; it is given by the following equation

$$\sigma_{k} = \sigma_{k+1} - \frac{(dz)_{min}}{H} \gamma^{k-1} \tag{18}$$

where $(dz)_{min}$, whose value is decided by the user, is the smallest spacing between the levels; the value of γ is calculated directly by the code;

iii) exponential distribution, as used in COMPLEX and in MC-3; if N is the number of the levels, then

$$\sigma_k = \frac{1}{e-1} \left[\exp\left(\frac{k-1}{N-1}\right) - 1 \right] \quad ; \tag{19}$$

iv) a distribution obtained through an additional coordinate transformation, as used by Moussiopoulos and Flassak [10]

$$\frac{k}{N} = \frac{1}{d} \left[(d+1)^{\sigma_k} - 1 \right] \quad (k = 0, 1, ..., N) ; \tag{20}$$

note that with $d \to 0$ the distance between sigma levels becomes constant and equal to 1/N; a value of d = 100, together with N = 10, was used by [10].

4.7. Typical grid dimensions and spacings

The variational calculus method has generally been used for simulating winds at the sub-synoptic scale. Thus, the dimensions of the region of application are typically from 10 to few hundred kilometres for horisontal extension and $1 \div 3$ kilometres for vertical extension.

In any case, in the choice of the exact boundaries of the area, it has to be remembered that there should be no terrain features outside the domain which could be expected to significantly influence winds within the domain.

The study of much larger areas may imply the separate simulation of their subareas. For instance, Parkinson [50] and Burch et al. [8, 51, 52] refer to a work performed to assess the economic wind energy resource in the UK. The NOABL model was used to calculate the wind field for 56 overlapping areas, each approximately $120 \ km \times 120 \ km$, covering the whole of the UK.

More recently, specific applications have been employed on much smaller and larger scales.

Röckle in his doctoral thesis [46] simulates the wind field around ingle houses, as well as in complex urban zones or on industrial estates.

At the other end of the spatial scale, Takeuchi and Adachi [43] have simulated an area of 300 km by 300 km, instrumented with more than 100 anemometers providing surface wind data.

Ishikawa [34] — with LSWIND, a model similar to MATHEW but including the effect of the earth's curvature — simulated an area of $3600~km \times 3600~km$ including most of Europe. The model was initialized with wind data coming from 171 surface and 101 aerological observations.

The maximum number of nodes depends on the characteristics of the computer, but to have a reasonable computation time it is advisable to avoid exceeding 10^5 nodes in the three-dimensional computational domain. In the more well known applications, as a consequence, the number of horisontal grid points varies from a minimum of 20×20 to a maximum of about 100×100 . Hence, horisontal spacing usually varies from a minimum of 50 m, as in [39, 40], to a maximum of 5 km, as in [53]. In the mentioned calculation of synoptic wind fields above Europe, the horisontal spacing is up to 72 km.

The top of the domain is usually placed between 1500 and 3000 m from the lowest height of the terrain; the number of conformal levels varies from 5 (see for instance [18]) to 20 (see for instance [11]).

5. THE INITIALIZATION PROCESS

5.1. General considerations

The process of initialisation \aleph (see section 1.1) is the set of operations that have to be performed on the N values of the wind vector, before imposing mass conservation. The aim of initialisation is to assign a value of wind speed and direction to all the grid points. The codes using Cartesian coordinates, such as MATHEW [14, 54] and WINDO4 [21, 2], and some of the models using conformal coordinates, such as COMPLEX

- [18, 19] and REDBL and the first version of CONDOR [10], use a four-step procedure
- i) the observed ind values are vertically extrapolated in order to obtain values at a reference height above ground level (e.g. $\sim 20 m$ in [14] and $\sim 5 m$ in [10]);
- ii) these values are interpolated at this height, usually with a $1/r^2$ law, using the nearest adjusted data (see section 5.4);
- iii) another 2D wind field is similarly obtained at the upper surface of the simulation volume;
- iv) finally, a vertical interpolation (see section 5.3) is performed between these two levels for every grid node.

In order to fill-in the computational mesh with the in ial guess, most of the models using conformal co-ordinates use the following two-step procedure

- i) measured or theoretical vertical profiles of the wind speed and direction are taken into account, if available; furthermore, a vertical profile of the wind speed and direction is obtained, using the extrapolation procedures discussed in section 5.3, at each location where surface observations exist;
- ii) once the vertical profiles are available, the wind speed and direction is interpolated (see section 5.4) in every horisontal plane, if Cartesian coordinates are adopted, or in every conformal surface.

In the BOLOS [23, 26] and WINDS [33] options using the geostrophic wind as the only input, a vertical profile is constructed at every grid point: no horisontal interpolation is then needed.

Chino and Ishikawa [2] observe that the accuracy of the predicted wind field greatly depends on the interpolation method of wind data. On the other hand, Troen [41] observes that:

- i) the density of the observational network is usually insufficient for resolving variations of the flow above complex terrain;
- ii) the quality of the available data is generally poor.

Therefore the interpolation based on all available data is meaningfull only if it is done between stations with:

- i) minimal influence of local topography;
- ii) good quality data.

For example, if a station is near an elevation or in a valley, the flow will be channelled almost independently from the flow in other areas. This effect is much stronger if the lower part of the PBL is stably stratified. The information from such a station will adversely influence the construction of the general flow above the area.

Chino and Ishikawa [2] – in the development of their SPEEDI (see the list of acronyms) – compared surface wind measurements performed in complex topography (one station on the a mountain peak (870 m a.s.l.), one

- on a ridge of the same mountain (350 m a.s.l.) and four at the base of the mountain) with upper winds measured using six pilot balloons. They found that
- i) wind direction and intensity at the peak coincide well with wind direction and intensity measured by the pilot balloons at the same height and thus represent the average airflow at the same elevation within a radius of at least 5 km;
- ii) a similar agreement is found between direction measurements at the ridge and data from the pilot balloons at 350 m, except when the top of the mountain creates a topographic barrier between the surface station and the balloon:
- iii) in many cases data from the peak station agree well with data from the ridge station;
- iv) data recorded at the base of the mountain do not agree well with data both at 350 and 870 m, mainly under light wind or calm conditions during day-break, sunset or night; the coincidence of data was better when the mixed layer was fully developed during the day.

As a consequence of their observations, Chino and Ishikawa devised an interpolation algorithm as reported in section 5.4.

Guo and Palutikof [32], testing the COMPLEX and NOABL codes, used wind data at one station (called the "predictor station") to predict wind speeds at the same station. They found that if the predictor station was low (high) in altitude relative to the general height of the test area, the models underpredicted (overpredicted) the wind speed, with differences between predictions and input data around 5% (20%). In order to partially overcome this limitation, Guo and Palutikof observe that if a wind field is mass-consistent, it will remain mass-consistent if all the wind speed components are increased or decreased by the same percentage. Thus, they multiply the predicted wind field by a certain scale factor to make the predicted wind speeds at the predictor station as close to their input values as possible. In an area with a number of predictor stations, Guo and Palutikof choose this scale factor to be the mean value of the ratios of the predicted to the observed mean wind speed at each station.

Finardi et al. [9], using MINERVE [28] to simulate the flow over two-dimensional hills, obtain a general flow underestimation when the wind profile used to initialize the code is the oncoming profile, and an overestimation when the profile located on the hilltop is added.

These considerations induced the authors of BOLOS [23, 26] and WINDS [33] to neglect the existing ground based measurements and initialise the models by providing only the geostrophic wind, in order to avoid data contamination in complex terrain and/or to supplement the scarcity of measurements.

We are convinced – and have verified – that it is possible to conclude that mass-consistent models allow experimental wind measurements taken simultaneously in a given area to be verified as follows. The measurements are used to generate a mass-consistent wind field. If, at a site, the simulated and the measured vectors differ greatly, while agreement is on average good, that particular measurement is likely to be affected by errors and/or very local effects.

The procedure, proposed by Boschetti et al. [55], to select the "exclusion areas", i.e. the areas unsuitable for siting anemometric stations, is based on similar considerations. These areas are selected as follows

- i) simulation of the wind field in a complex topography, under different wind directions and intensities and under different stability conditions, using a mass-consistent model;
- ii) identification of nodes in which, under one or more simulated conditions, the wind vector differs greatly from the wind vector which would have resulted, at the same node and at the same distance from the terrain, in the case of a flat and homogeneous land.

5.2. Different types of data utilised

Usually mass-consistent wind models accept wind data from one or more of the following observation types:

- i) surface meteorological stations recording at a single height (usually $\sim 10 m$ above ground level);
- ii) meteorological towers recording at different heights;
- iii) vertical soundings from wind profilers, balloons, etc.; and
- iv) gradient or geostrofic wind.

Some models use only surface measurements (MAS-CON [13]), others can also use the geostrophic wind and one (MATHEW [14]) or more observed wind profiles when available. NOABL accepts surface measurements and/or one vertical profile.

Troen [41], as a consequence of his observations about problems arising when interpolating (see section 5.1), suggests that the input data should be either one "good" surface observation or an upper air observation.

As already stated, EOLOS [23, 26] and WINDS [33] have the option of accepting only the geostrophic wind intensity and direction as an input.

If the sea level pressure is available at three stations that form a triangle, the centre of which is near the site, Endlich et al. [19] and Guo and Palutikof [32] calculate the geostrophic wind from this information. If pressure data are not available, Guo and Palutikof assume an upper-level wind speed value of 2.8 times the average surface wind speed, while the average surface wind direction with 40^o veering is used as the wind

direction at the top of the boundary. The geostrophic speed is applied by Endlich [20] as a height between 500 m (smooth terrain) and 900 m (rough terrain) above ground level.

Takeuchi and Adachi [43] deduced the geostrophic wind, assumed to be such at above $\sim 2000 \, m$ a.s.l., from the sea surface pressure, interpolating between observations at meteorological stations using the least squares method with a 10 parameter analytical expression.

Kitada et al. [48] claim that data from at least three observation locations are required to reproduce a land/sea breeze circulation. The horizontal wind data should also be known in the upper layers. Furthermore, one of servation location should be in the region of the maximum variation of the horizontal wind field.

Finardi et al. [9], in their simulation of the flow over two-dimensional hills, find that neither MATHEW nor MINERVE are able to describe the wind field, mainly in the wake region, using only 1 or 2 vertical wind profiles as input. When 3 vertical wind profiles are used as input data, the flow is well depicted everywhere except in the lee. In the steepest considered hill, where a stationary separated sone exists, the input of 4 profiles (2 in the lee and 2 upwind of the peak) allows a description to be made of the main features of the flow. A good result is also obtained, in this case, by increasing the height of the terrain in the lee up to the level of zero wind (obtained from data), thus excluding the counterflow area.

The problem of simulating flow separation is even more important in the simulation of wind flow around buildings. Röckle [46] modifies the initial field around each building using rules deduced from experimental situations.

Bocciolone et al. [56] simulate wind fields in the Straits of Messina, Italy, with a mass-consistent code having a resolution of $\sim 1200\,m$ and initialised with a number of different geostrophic winds. They then correct the outputs of the code using a two-dimensional code which takes into account, in vertical planes, the effect of roughness changes and small topographic irregularities in the vicinity of the anemometers located in the considered area. Finally, these corrected values of the wind speed and direction are compared with the actual anemometric measurements.

5.3. Vertical extrapolation

5.3.1. Constant profiles

Only MASCON [13] utilises a vertically averaged value of wind speed within the boundary layer. This value is deduced as the mean value calculated over a power law profile

$$\overline{u} = \frac{u_1}{z_{bl}} \int_{z_1}^{z_{bl}} (z/z_1)^p dz$$
 (21)

where z_{bl} is the height of the inversion base above orography, u_1 and z_1 are the speed of the measured wind and the height at which the measurement has been performed respectively, and $p \sim 1/7 \sim 0.14$.

The wind profile is usually assumed – in models using the power law (see section 5.3.3) within the Surface Layer (SL from here on) – to be constant from the top of the SL to the top of the domain.

Usually, the wind in the free atmosphere is assumed to be constant with height. This assumption is made, for instance, by Troen [41], by Takeuchi and Adachi [43] and by Ratto et al. [33].

5.3.2. Linear profiles

The codes MATHEW, NOABL and REDBL and the first version of CONDOR (see [10]) allow a linear interpolation, to be used above the SL, with the geostrophic wind, if available, at the top of the planetary boundary layer.

5.3.3. Power law

One of the wind profiles used in the oldest mass-consistent models is the power law. This is used: in MATHEW by Sherman [14] (in the SL), in NOABL [15-17], by Bhumralkar et al. [18], by Kitada et al. [1] (up to 500 m), by Kitada et al. [48], by Moussiopoulos and Flassak [10] and by Ishikawa [21, 34] (below the SL).

Its form is

$$u(z) = u_1 \left(\frac{z}{z_1}\right)^p \quad z < z_{il} \tag{22}$$

where p, z_1 and u_1 are the same quantities as in equation (21) and z_{sl} is the SL height. In the mentioned models z_{sl} is assumed to be $100 \sim 200 \ m$. It should be noted that p depends in a complex way on atmospheric stability ($p \sim 0.14$ in neutral conditions), on the roughness length z_o and on wind speed.

Although very widely used, expression (22) has strong limits, mainly linked to the dependence of p on the quantities mentioned above. Moreover, the power law is an empirical law, and its validity is limited to the lowest 10% of the boundary layer, i.e. to the SL.

Takeuchi and Adachi [43] assume a power law profile for wind speed and a linear law for wind direction from 50 m above ground level to the top of the boundary layer.

Troen [41], Lalas [23, 26] (EOLOS model) and Ratto et al. [33] (WINDS model) calculate the wind between the top of the SL and the bottom of the free layer through an interpolation scheme

$$u(z) = u_{sl}(z) + \alpha(z) [u_G - u_{sl}(z)]$$

$$v(z) = \alpha(z) v_G$$
 (23)

where $u_{sl}(z)$ is the wind speed in the SL, u_G and v_G are the x and y components of the geostrophic wind

and $\alpha(z)$ is a third order polynomial such that, where

$$\alpha(z_o) = \alpha'(z_o) = \alpha'(z_{bl})$$
 $\alpha(z_{bl}) = 1$

where z_{bl} is the PBL height. Note that here the x axis is taken parallel to the wind in the SL.

5.3.4. Logarithmic profiles

When upper wind data are available, Endlich et al. [19, 20], Ishikawa [21, 34] (above the SL), Kitada et al. [48] and Georgieva [44] interpolate vertically between the surface data and the wind at the top of the domain using the law

$$u = a \log z + b$$
$$v = c \log z + d$$

which permits the wind to change both in direction and in speed with height.

Furthermore, Guo and Palutikof [32] incorporated in MC-3 a procedure to adjust the wind speeds assuming a logarithmic profile and allowing for variable surface roughness in the environment close to the masts for 30° sectors around the mast itself.

Takeuchi and Adachi [43] assume a logarithmic law for wind speed and a costant wind direction in the first 50 m above ground level.

Troen [41], Lalas [23, 26] and Ratto et al. [33] also introduce logarithmic or log-linear profiles

$$\overline{u}(z) = \frac{u_*}{k} \left[\log \frac{z}{z_0} - \psi_m \right] \quad z_o < z < z_{sl} \tag{24}$$

where u_n is the friction velocity, k is Von Karman's constant (its experimental value is about 0.4), z_0 is the roughness length and z_{sl} is the height of the SL. Since these expressions are valid only for the lowest 10% of the PBL, the models using them adopt the interpolation formula (23) above the SL.

Codes using logarithmic and log-linear profiles have the advantage of allowing the effect of roughness on wind intensity and direction to be taken into account.

WINDS [33] allows other formulae to be used that give the profile for the whole boundary layer and consider the dependence of the profile on stability and roughness. These were deduced by Zilitinkevich [57] and have the form

$$\overline{u}(z) = \frac{u_*}{k} \left[\log \frac{z}{z_o} + a_\mu \left(\frac{z - z_o}{z_{bl}} \right) + a_\mu^* \left(\frac{z - z_o}{z_{bl}} \right)^2 \right]$$

$$\overline{v}(z) = -\frac{u_*}{k} \left[b_\mu \left(\frac{z - z_o}{h} \right) + b_\mu^* \left(\frac{z - z_o}{h} \right)^2 \right]$$

where the empirical coefficients b_{μ} , b_{μ}^{*} , a_{μ} and a_{μ}^{*} depend on a stability parameter μ related to the Monin

length and are chosen in order to match (25) with (24) in the SL.

5.3.5. Observed profiles

If an observed wind profile is available (i.e. several measurements at different heights above the same terrain point, covering all or a fraction of the height of the simulation domain), it can be used in some of the codes (for instance in NOABL, EOLOS, WINDS and ATMOS1) to calculate the first guess field.

Hiester and Pennel [58] introduce a linear interpolation between a rawinsonde sounding, if available, and surface wind data such that the initial field has the same speed and direction as the surface wind near ground, and the wind aloft at the top of the domain.

Davis [22], with his code ATMOS1, has sometimes used calculated drainage flow profiles, instead of vertical profiles deduced from surrounding wind soundings.

5.3.6. Unidimensional model profiles

When more simulations are required at different hours of the day, but only an observed profile at the initial time is available, the successive wind profiles can be calculated, as done by [59], with a hydrodynamic time-dependent unidimensional model of the PBL. Here, unidimensional means that the model simulates the PBL vertical structure, but gives no information at all about horisontal variation of the wind. The coupling with a mass-consistent model will produce an account of the terrain-induced perturbations of the flow.

5.4. Horisontal interpolation

To extend the available vertical profiles to all the grid points, mass-consistent models usually interpolate the values at a certain discretization level ($z = \cos t$ or $\sigma = \cos t$ in Cartesian or conformal coordinates respectively), with the rule

$$(u^{o}, v^{o}) = \frac{\sum_{j=1}^{N} (u, v)^{j} f(r_{j})}{\sum_{j=1}^{N} f(r_{j})} . \tag{26}$$

Here (u^o, v^o) and $(u, v)^j$ are the x and y components of the wind vector to be calculated and the x and y components of the wind vector along the j-th profile respectively, r_j is the distance between the point of known value $(u, v)^j$ and the point at which (u^o, v^o) is being calculated, and f is a weighting factor.

The sum is usually extended either to the nearest (typically N=3) measurements or to the measurements included in a region surrounding each grid point, with a limited "radius of influence" R. In the analysis of a two-dimensional land/sea breeze circulation, Kitada et al. [1] found that a radius R=L/N, where L is the length of the horisontal region and N is the number of observations, gave slightly better results than

R=L. The same authors, in the analysis of a three dimensional land/sea breeze circulation, used a radius about twice the average separation distance between observation points.

The most frequently used weighting factors are

$$f(r_j) = (1/r_j)^2 (27)$$

Otherwise

$$f(r_i) = exp \left(-r_i/R_o\right)^2 \tag{28}$$

as used in MASCON [13] and by Chino and Ishikawa [2], who assume $R_o^2 \sim 10 \ km^2$. Factor (28), with respect to factor (27), has the advantage of eliminating the complete dominance of a measuring station near a grid point. The model CONDOR [11] can use either of the weight-functions considered above or a combination of both.

Kitada et al. [1] also used the 1/r weighting function in their reconstruction of a two-dimensional land/sea breeze circulation, finding an adjusted wind field much too smooth for a wind field with strong local characteristics.

Chino and Ishikawa [2], following their analysis of wind measurements performed in complex topography (see section 5.1), replaced the weighting factor $f(r_j)$ with the product

$$f = f(r_i)f(\Delta z)f(\Delta z_b)$$

where r_j is the same horisontal distance as in (26), Δz is the vertical distance between the two considered points and Δz_b is a vertical distance related to the height of the barrier separating the two points. The factor $f(\Delta z)$ has a structure such that

- i) the weighting of the station on the peak with respect to the lower grid points decreases slightly with their vertical distance, except for the grid points in the vicinity of the base of the mountain;
- ii) the weighting of the surface stations with respect to the higher grid points decreases rapidly with their vertical distance.

The factor $f(\Delta z_b)$ has a structure such that the weighting of a station in complex terrain with respect to a grid point decreases when a barrier separates them.

6. NUMERICAL SOLUTION OF DIFFER-ENTIAL EQUATIONS

Sherman [14], Adell et al. [54] and Ishikawa [21, 34] solve a discrete formulation of equation (8) written in Cartesian coordinates with respect to λ , with the boundary conditions discussed in section 2.2. The

equations are solved iteratively using a successive overrelaxation method (see Appendix C). The adjusted velocity field is then calculated using a discrete formulation of equations (6).

A difference between these approaches consists of the fact that Sherman [14] and Adell et al. [54] estimate all variables at the grid points, while Ishikawa [21, 34] uses a staggered grid. In this second approach, scalar quantities such as λ are estimated at the centre of the mesh while components of vectorial quantities are calculated at the centres of the sides of the same meshes.

Both the COMPLEX model [18-20] and the MC-3 model [32] assume that the flow is parallel to the terrain-conformal surfaces, with no flow through them. In other words, in these models the flow is assumed non-divergent in any layer defined by conformal surfaces, independently of the flow in neighbouring layers. At the same time, a procedure is adopted to preserve the vertical vorticity in each computational cell. Instead of applying the variational calculus to the whole domain, the layers of the grid can be treated in sequence. This makes the computations simpler and more efficient than three-dimensional relaxation.

Guo and Palutikof [32] observe that this artifice reduces the computing time of a wind pattern by a factor six. On the other hand, these same authors also find that the topographic adjustments introduced by COMPLEX [18-20] to the wind speeds are insufficient: the model tends to underestimate (overestimate) wind speeds over relatively high (low) ground. This does not necessarily imply that the other code examined (NOABL) is, in all circumstances considered by Guo and Palutikof, superior to COMPLEX in its predictive capacity.

Endlich et al. [19] and Hiester and Pennel [58] claim that the terms neglected in COMPLEX model, for the sake of reducing computation time, may be significant in areas of steep terrain.

Almost all other codes numerically solve the discrete formulation of equation (8), written in terrain conformal coordinates, by using successive overrelaxation. Once λ is known, a discrete formulation of equations (6), rewritten in conformal coordinates, yields the adjusted velocities at the model grid points.

Moussiopulos and Flassak [10] solve the discrete formulation of the elliptic equation (8) with two different algorithms, devised to achieve a full vectorisation on vector computers like the CYBER 205. The first algorithm consists of a fast direct elliptic solver, based on the use of finite Fourier transforms, applied together with the block iteration technique (code CONDOR). The second is the so called Red-Black Successive Overrelaxation Method (code REDBL).

Moussiopulos et al. [11, 60], presenting the refined version of their code CONDOR, claim the superiority

of substituting a discrete formulation of the Euler-Lagrange equations (6) into the discrete formulation of the continuity equation (2) to yield a discrete formulation of the elliptic equation. This approach, using a 25-point-operator instead of a 15-point-operator, guarantees a better reduction of the wind field divergence. The discrete formulation of the elliptic equation is then solved with an algorithm based on the Fourier analysis applied in two directions. This algorithm is an application of Fast-Fourier-Transformation and full vectorization (see also [61, 27]).

7. MODEL TESTING

tuning and testing.

Barnard et al. [39] observed that a difficulty that has beset the mass-consistent models is lack of verification

Verification studies using data taken from the island of Oahu, Hawaii [62] and the Nevada Test Site [63] have shown that the root-mean-square error between calculated and observed winds is typically 2 to 4m/s. Barnard et al. [39] applied an optimisation technique to the mass-consistent model NOABL. Eight sets of hourly averaged wind data were available for model

Within this approach, a very simple initialisation was performed where only one site (the station with the highest average wind speed, called the "reference site") was used to initialise the model. Subsequently, the error between the calculated winds and the observed winds at six to eight "tuning sites" formed a basis for gauging the model's performance. The stability parameter α and the initial wind direction were then adjusted until this error was minimized. Finally, optimum parameters were used to calculate the wind in the remaining (~ 20) "verification sites".

When the optimum parameters were used by Barnard et al. [39, 40] to calculate the winds over the modelled area, the model produced good results for six out of the eight datasets. In these cases, the root-mean-square errors between the calculated and observed wind speed ratios (the wind speeds are normalised by the reference site wind speed) were less than 0.08 for verification sites and less than 0.06 for tuning sites. The two cases that did not perform well were those involving low wind speeds.

Guo and Palutikof [32], in their testing of COMPLEX, NOABL and MC-3 already presented in section 5.1, concluded that the predictions strongly depend on the values given to parameters such as PBL height and then on decisions heavily influenced by the judgement of individual users.

Walmsley et al. [24] tested three JH based models (Mason-King, MS-Micro and BZ-WASP) and the mass-consistent model EOLOS using field measure-

ments performed at Blashaval Hill [64]. These authors found that discrepancies between the different models were minor, although Eolos was in somewhat worse agreement with measurements, especially away from the summit of Blashaval Hill. For most wind directions, errors in normalized wind speed at the summit were 7% or less.

Ross et al. [29] tested the capability of NUATMOS to simulate analytical solutions for potential flows around simple objects (a hemisphere, a half cylinder and half ellipsoids with various aspect ratios) in neutral conditions and with only background wind information available.

Ros. et al. [31] subjected their code NUATMOS to a systematic testing using meteorological data from the Rocky Flats in Colorado, USA. They simulated a volume of roughly $150 \times 150 \times 5.5 \ km^3$, including the Denver metropolitan area and a portion of the Rocky Mountains, with a $151 \times 161 \times 9$ grid. More precisely, wind observations from 17 surface meteorological stations and 300 meteorological cases were provided as input to the code. These authors evaluated

- i) the ability of the code to preserve input wind observations; model performance was assessed by comparing the resulting distribution of wind speed and wind direction (predicted observed) differences at the considered stations, (for a total of 4354 useable data points);
- ii) the ability of the code to predict wind observations; model performance was assessed by comparing the resulting distribution of wind speed and wind direction (predicted observed) differences at 10 additional surface meteorological stations and 6 profilers, each reporting at the 200 m, 900 m and 2000 m levels (for a total of 6918 useable data points).

The ability of NUATMOS to preserve input wind observations is confirmed by a tendency to adjust input wind speeds slightly downward, the median wind speed difference being $\sim -0.3~m/s$, the mean $\sim -0.4~m/s$ and the inter quartile range (IQR) $\sim 0.6~m/s$; the corresponding quantities for the wind direction difference being $\sim +1.4$ degrees, $\sim +2.1$ degrees and ~ 11.2 degrees.

These figures, in testing the ability of the code to predict wind observations, become ~ -1.3 m/s, ~ -1.4 m/s and ~ 3.4 m/s and $\sim +10.8$ degrees, $\sim +10.2$ degrees and ~ 66.5 degrees respectively.

These results are favourably compared with those obtained with a two-dimensional diagnostic wind field model called WINDS, not to be confused with the WINDS model described in this paper.

Finardi et al. [9], use two mass-consistent codes (MATHEW [14] and MINERVE [28]) and two dynamic linearised models (MS3DJH/3R and FLOWSTAR) to simulate the flow over two-dimensional hills of analyti-

cal shape and varying slope. The results are compared with detailed wind tunnel data by Snyder [65]. Different numerical experiments have been performed, varying the value of the stability parameter α and input data (the complete data set, i.e. 15 wind profiles, 3 profiles, the encoming wind profile plus two measurements taken near the ground). Their conclusions, about the ability of a mass-consistent code to describe the main features of a wind field over complex terrain depending on the availability of input data, have been already reported in section 5.2.

8. CONCLUSIONS

The aim of this work was to highlight all the options and improvements introduced in mass-consistent models since their conception, their present state and, in particular, the solutions provided for each single problem.

It is our opinion that these models, even though the physics involved is very simple, can be further developed and improved. The improvements can be obtained for instance through the parametrisation of stability (see section 3) or by using the telescoping procedure (see section 4.5). Furthermore, our research group is obtaining encouraging results from "nesting" a mass-consistent model in the output of a prognostic model operating at a larger scale.

There are, undoubtly, intrinsic limitations that cannot be eliminated in mass—consistent models, such as the lack of dynamic properties: the principal weakness of this approach. These models however provided performances at least equal to the more sofisticated models in several applications. This fact, together with the efforts made by many people to obtain the improvements we mentioned above, shows that research on the mass—consistent approach and practical use of such codes are still in course.

Acknowledgements

This text is partially based on the lecture given in 1990 by C.F. Ratto at the International Centre for Theoretical Physiscs, Trieste, Italy. Illuminating discussions and correspondences with G. Brusasca, D.P. Lalas, G. Lo Vecchio, A. Massino, J. Moussafir, N. Moussiopulos, H. Ishikawa, F. Tampieri, I. Troen and G. Zanini are gratefully acknowledged.

APPENDICES

A. LIST OF ACRONYMS

CONDOR	Calculation Of NonDivergent wind fields Over Rough terrain
MASCON	MASs CONsistent wind field
MATHEW	Mass-Adjusted THrEe-dimensional Wind
MC-3	Mass Consistent 3-rd code
NOABL	New Objective Analysis of
	Boundary Layer (our guess)
REDBL	RED-Black successive overrelaxation
SPEEDI	System for Prediction of Environmental
	Emergency Dose Information
WINDS	Wind field Interpatation by
	Non Divergent Schemes
WSPEEDI	regionally extended/Worldwide version of SPEEDI

B. STATISTICAL TREATMENT OF THE DATA

Some researches may be more concerned with the statistical properties of the wind rather than with wind flow at a fixed moment. This is evident if we consider that an important application of these models relates to the siting of WECS and the evaluation of their potential.

Two procedures can be followed to extract statistical properties from a time series of wind data

- i) calculation of statistical properties of the available measurements (mean value, frequencies of the data, etc.) then applying the model with the obtained values;
- ii) application of the model for every measurement and then extract statistical properties of the time series of wind flows.

A few methods have been devised that allow a saving in computational time without losing fundamental information. All these methods use the linearity of the processes involved in the models (interpolation schemes, numeric solution processes, etc). The following paragraphs examine Traci's method, the eigenvector method and Lalas' method.

B.1. Traci's method

Traci's method [15, 58] consists of examining available data and constructing important categories of flow conditions and their frequency of occurrence.

This method has been used to analyze the set of measurements collected at Oahu, Hawaii; measurements were made over a 24-month period. The idea of Traci's method is that only one day for each month is chosen as representative of the month itself. The criteria used to choose representative data are strongly subjective

and thus not obvious.

This method allows the extraction of some data from a large data set. This is sometimes a great advantage, since it can be impossible to run the model for the entire data set. It should be never forgotten, however, that the validity of the result depends on the representative nature of the data chosen.

The Property of Street Book of the Street

B.2. The eigenvector method

This method is used in COMPLEX [18-20] and was presented for the first time by Ludwig and Byrd [66].

The model utilizes the linear characteristics of mass-consistent models by combining solutions from the eigenvectors of the covariance matrix of the wind component data. This method was demonstrated to be practical and economic for the applications considered. Nevertheless, according to Ross et al. [29], it does not appear to be suitable for dealing with large datasets, especially when vertical wind profiles are available, due to the large number of eigenvectors to be considered.

Let us suppose we want to calculate the wind flow over a region at a given hour: the input is represented by m wind data from N stations on the surface. As the model needs both horisontal components of the velocity, the number of data is $2N \times m$. Let $v_{ik}(i=1,...,2N;k=1,...,m)$ be the data matrix. Then

$$\overline{v}_i = \frac{1}{m} \sum_{k=1}^m v_{ik}$$

is the mean value of the *i-th* row of this matrix (i.e. it is the time average of the measurements at a fixed station and for a fixed component).

Now let $\vec{v}^{(k)}$ be a vector (with 2N components) representing the measurements at all the stations at a fixed time k (i.e. a column of the v_{ik} matrix) and then let

$$\vec{v}^{(k)} = a_1^{(k)} \vec{e}_1 + \dots + a_{2N}^{(k)} \vec{e}_{2N} + \overline{\vec{v}}$$
 (29)

be the decomposition of this vector on the base of the eigenvectors $\vec{e}_1 \div \vec{e}_{2N}$ of the covariance matrix,

$$C_{ij} = \sum_{k=1}^{m} (v_{ik} - \overline{v}_i)(v_{jk} - \overline{v}_j) \quad (i, j = 1, 2, ..., 2N) .$$

Thanks to the linearity of the model, the decomposition (29) allows the model to be run only 2N + 1 times (a number that is usually around ten). If $\vec{e_1}^{sol}, \dots, \vec{e_{2N}}^{sol}, \vec{v}^{sol}$ is the output of the model corresponding to input $\vec{e_1}, \dots, \vec{e_{2N}}, \vec{v}$, then the output for the generic input vector $\vec{v}^{(k)}$ is

$$\vec{v}^{(k)}$$
 sol = $a_1^{(k)}\vec{e}_1^{\ sol} + \dots + a_{2N}^{\ (k)}\vec{e}_{2N}^{\ sol} + \overline{\vec{v}}^{\ sol}$

where the coefficients $a_1^{(k)}, ..., a_{2N}^{(k)}$ are those of the decomposition (29). Note that the time required for

their calculation is much smaller than the time needed for a single run. Consequently, once the model has been applied for the eigenvectors and the time average vector, the remainder of the simulation is very quick.

B.3. Lalas' method

Lalas's method [3] is used when the code can be initialized with the geostrophic wind only (i.e. EOLOS and WINDS).

Wind data are classified according to their speed i, direction j and day/night occurrence k (which gives a rough estimation of stability conditions): frequencies of occurrence are thus calculated and stored in the matrix f_{ijk} . The model then runs for a fixed geostrophic intensity (usually chosen as equal to $10 \, m/s$), direction j and condition k. Then, at the grid point (x, y) a wind speed $\vec{v}_{jk}(x, y)$ is obtained. This operation is repeated for all the j and k values.

Thanks to the linearity of the model, the mean wind speed can then be calculated as

$$\overline{v(x,y)} = \sum_{k=1}^{2} \sum_{j=1}^{j_{max}} \sum_{i=1}^{i_{max}} \left[\frac{G_i}{10} f_{ijk} v_{jk}(x,y) \right]$$
(30)

where G_i is the geostrophic wind speed corresponding to i-th class. Obviously, the average is annual, seasonal, monthly, etc. depending on the averaging period used to obtain f_{ijk} .

The energy flux through a unit surface normal to the flow can also be calculated as

$$\overline{P(x,y)} = \frac{1}{2}\rho \sum_{k=1}^{2} \sum_{j=1}^{j_{max}} \sum_{i=1}^{i_{max}} \left[\left(\frac{G_i}{10} \right)^3 f_{ijk} v_{jk}^3(x,y) \right]$$
(31)

where ρ is air density.

C. THE OVERRELAXATION METHOD

For investigating iterative solution methods of large systems of equations, it is convenient to analyse the problem in its vectorial form

$$A\Phi = f \tag{32}$$

A being the coupling matrix of the system, Φ the vector whose components are the unknowns and f the vector which contains, among other terms, the right hand side of equation (8).

In an iterative scheme, the solution for the Φ vector is obtained by the calculation of

$$\Phi^{i+1} = \Phi^i - \tau (A\Phi^i - f) \tag{33}$$

where Φ^i is the "old" value of the Φ vector, which has been calculated in the preceding iteration, and Φ^{i+1} is

the "new" value (which will take the place of Φ in the next iteration). τ is a parameter on which most of the effectiveness and convergence rate of the solution depends; it may vary with iterations, but is often chosen as a constant.

As a result of the aknowledged importance of the τ parameter, great effort has been made to evaluate its best value. For the general (and simplest) case, this is found to be

$$au = \frac{1}{\beta}$$

 β being the largest eigenvalue of the A matrix.

In many problems of mathematical physics (including ours, i.e. the solution to equation (8)) a more efficient method can be used, i.e. one that converges quicker: the "overrelaxation method". This can be used if the A matrix has the tridiagonal form

$$\begin{pmatrix} 1 & -T_1 & 0 & 0 & \dots & 0 & 0 \\ -S_2 & 1 & -T_2 & 0 & \dots & 0 & 0 \\ \dots & \dots & \dots & \dots & \dots & \dots & \dots \\ 0 & 0 & 0 & 0 & \dots & -S_k & 1 \end{pmatrix}$$

In this case, the A matrix can be written as

$$A = E - S - T$$

where

$$T = \left(\begin{array}{cccccc} 0 & T_1 & 0 & \dots & 0 & 0 \\ 0 & 0 & T_2 & \dots & 0 & 0 \\ \dots & \dots & \dots & \dots & \dots & \dots \\ 0 & 0 & 0 & \dots & 0 & 0 \end{array} \right) \quad \text{,}$$

and

$$S = \left(\begin{array}{ccccccc} 0 & 0 & 0 & \dots & 0 & 0 \\ S_2 & 0 & 0 & \dots & 0 & 0 \\ \dots & \dots & \dots & \dots & \dots & \dots \\ 0 & 0 & 0 & \dots & S_k & 0 \end{array} \right) \quad ,$$

and E is the unit matrix.

It can be shown that in this case the optimal value for τ is

$$\tau = \omega = \frac{2}{1 + \sqrt{1 - \beta^2}} \tag{34}$$

 β being the largest eigenvalue of the matrix B = S + T.

In order to apply the overrelaxation method to mass-consistent models, equation (8) is solved on a single "column" of the domain (i.e. all the cells with fixed i and j). This process is then repeated for all the columns and for a certain number of times, until the desired degree of approximation is reached.

⁶In this way the A matrix has the form described above.

List of most frequently used symbols

$a_\mu, a_\mu, a_\mu^*, b_\mu^*$	coefficients in Zilitinkevich profiles
E(u, v, w)	functional representing the difference
_	between initial and adjusted fields
Fr	Froude number
h 	height of terrain
H	height of the domain
\mathcal{H}	characteristic height difference
H_a H_c	average thickness of the PBL at a site
11 _C	height of the critical streamline in stable flows
St	procedure of adjustment of the
Ü	wind field
J(u, v, w)	functional to be minimized
k	Von Karman constant
\vec{n}	unit vector normal to the surface
	of the domain
N	number of stations
N	buoyancy frequency
Я	procedure of initialization of the
	wind field
p	exponent in the power law
u, v, w	components of the wind field \vec{V}
ũ, v, ŵ	components of the wind field
	in conformal coordinates
$\boldsymbol{u}^{o}, \boldsymbol{v}^{o}, \boldsymbol{w}^{o}$	components of the wind field \vec{V}^o
u_G, v_G	components of geostrophic wind
<i>U</i>	velocity scale or characteristic
	wind speed
u. 17∕	friction velocity
^V V°	adjusted wind field
$ec{V}_i$	initial or "first guess" wind field
-	measured wind vector at i-th station
x, y, z	Cartesian coordinates height of the PBL
z _{bi}	height of the SL
z_o	roughness length
α	ratio between weights $\alpha_1 = \alpha_2$ and α_3
$\alpha(z)$	polynomial used to interpolate between
` '	geostrophic and SL wind
$\alpha_1 = \alpha_2$	Gauss precision modulus relative to
	horisontal wind speed adjustments
α_3	Gauss precision modulus relative to
	vertical wind speed adjustments
r	surface of the domain \(\Omega \)
$\delta \vec{V}$	first variation of the velocity at a boundary
Δz	vertical distance between two points
Δz_b	vertical distance related to the height
	of a barrier separating two points
λ	Lagrange multiplier
μ	stability parameter
ρ	air density
σ	height above terrain in conformal
	coordinates

σ_i	variance of the i-th component
•	of the wind vector
θ	potential temperature
au	transmissivity or empirical stability
	parameter
τ_h	horizontal transmissivity
$ au_{v}$	vertical transmissivity
ζ	z-component of vorticity
ξ, η, σ	conformal coordinates
ψ_m	function in log-linear profiles
Ω	domain of the simulation

REFERENCES

- T. Kitada, A. Kaki, H. Ueda, and L.K. Peters. Estimation of vertical air motion from limited horizontal wind data A numerical esperiment. Atmos. Environ., 17:2181-2192, 1983.
- M. Chino and H. Ishikawa. Experimental verification study for System for Prediction of Environmental Emergency Dose Information; SPEEDI, (I). Three-dimensional interpolation method for surface wind observations in complex terrain to produce gridded wind field. J. Nucl. Sci. Technol., 25:721-730, 1988.
- D.P. Lalas. Wind energy estimation and siting in complex terrain. Int. J. Solar Energy, 3:43-71, 1985.
- P.S. Jackson and J.C.R. Hunt. Turbulent wind flow over a low hill. Q. J. R. Meteorol. Soc., 101:833-851, 1975.
- R. Pielke. Mesoscale Meteorological Modeling. Academic Press, Inc., Orlando, Florida, 1984.
- N. Dinar. Mass consistent models for wind distribution in complex terrain. Fast algorithms for three dimensional problems. Bound. Layer Meteorol., 30:177-199, 1984.
- W.T. Pennel. An evaluation of the role of numerical wind field models in wind turbine siting.
 Technical Report PNL-SA-11129, Battelle Memorial Institute, Pacific Northwest Laboratory, Richland, Washington, 1983.
- S.F. Burch and F. Ravenscroft. Computer modelling the UK Wind Energy Resource: Final Overview Report. Technical Report ETSU WN 7055, AEA Industrial Technology Harwell Laboratory, 1992.
- S. Finardi, G. Brusasca, M.G. Morselli, F. Trombetti, and F. Tampieri. Boundary-layer flow over analytical two-dimensional hills: a systematic comparison of different models with wind tunnel data. Bound. Layer Meteorol., 63:259-291, 1993.
- N. Moussiopoulos and Th. Flassak. Two vectorised algorithms for the effective calculation of mass-consistent flow fields. J. Climate Appl. Meteor., 847-857, 1986.
- 11. N. Moussiopoulos, Th. Flassak, and G. Knittel. A

- refined diagnostic wind model. Environ. Software, 3:85-94, 1988.
- Ib Troen. C diagnostic wind field models. In D.P. Lalas and C.F. Ratto, editors, Modelling of Atmospheric Flow Fields. Lectures given at the International Centre for Theoretical Physics, Trieste, Italy, World Scientific Publishing Co. Ltd., 1994.
- M.H. Dickerson. MASCON A mass consistent atmospheric flux model for regions with complex terrain. J. Appl. Meteor., 17:241-253, 1978.
- C.A. Sherman. A mass-consistent model for wind fields over complex terrain. J. Appl. Meteor., 17:312-319, 1978.
- R.M. Traci, G.T. Phillips, P.C. Patnaik, and B.E. Freeman. Development of a wind energy site selection methodology. Technical Report RLO/2440 11, NTIS U.S. Dept. of Energy, 1977.
- R.M. Traci, G.T. Phillips, and P.C. Patnaik. Developing a site selection methodology for wind energy conversion systems. Technical Report, DOE/ET/20280-79/3. NTIS, Science Applications Inc. Springfield, Virginia, 1978.
- G.T. Phillips. A preliminary users guide for the NOABL objective analysis code. Technical Report DOE Contract AC06-77/ET/20280, NTIS U.S. Dept. of Energy, Springfield, Virginia, July 1979.
- C.M. Bhumralkar, R.L. Mancuso, F.L. Ludwig, and D.S. Rennè. A pratical and economic method for estimating wind characteristics at potential wind energy conversion sites. Solar Energy, 25:55– 65, 1980.
- R.M. Endlich, F.L. Ludwig, C.M. Bhumralkar, and M.A. Estoque. A diagnostic model for estimating winds at potential sites for wind turbines. J. Appl. Meteor., 21:1442-1454, 1982.
- R.M. Endlich. Wind energy estimates by use of a diagnostic model. Bound. Layer Meteorol., 30:375-385, 1984.
- H. Ishikawa. A computer code which calculates three-dimensional mass-consistent wind field. Technical Report JAERI-M 83-113, Japan Atomic Energy Research Institute, 1983. (In Japanese).
- C.G. Davis, S.S. Bunker, and J.P. Mutschlecner. Atmospheric transport models for complex terrain. J. Climate Appl. Meteor., 23:235-238, 1984.
- 23. D.P. Lalas, M. Tombrou, and M. Petrakis. Comparison of the performance of some numerical wind energy siting codes in rough terrain. In European Community Wind Energy Conference, Herning, Denmark, 6-10 June 1988.
- J.L. Walmsley, Ib Troen, D.P. Lalas, and P.J. Mason. Surface—layer flow in complex terrain: comparison of models and full-scale observations. Bound. Layer Meteorol., 52:259-281, 1990.
- 25. C.F. Ratto. The AIOLOS and WINDS codes.

- In D.P. Lalas and C.F. Ratto, editors, Modelling of Atmospheric Flow Fields. Lectures given at the International Centre for Theoretical Physics, Trieste, Italy, World Scientific Publishing Co. Ltd., 1994.
- 26. M. Tombrou and D.P. Lalas. A telescoping procedure for local wind energy potential assessment. In W. Palz, editor, Resource assessment. European Community Wind Energy Conference, H. S. Stephens & Associates, Madrid, 1990.
- 27. Th. Flassak and N. Moussiopoulos. An efficient diagnostic wind model for the calculation of air flow in rough terrain. In 2nd International Conference on Atmospheric Science and Applications to Air Quality, Tokyo, October 3-7 1988.
- P. Geai. Methode d'interpolation et de reconstitution tridimensionelle d'un champ de vent: le code d'analyse objective MINERVE. Technical Report DER/HE/34-87.03, EDF, Chatou, France, 1985.
- D.G. Ross, I.N. Smith, P.C. Manins, and D.G. Fox. Diagnostic wind field modeling for complex terrain: model development and testing. J. Appl. Meteor., 27:785-796, 1988.
- D.G. Ross and D.G. Fox. Evaluation of an air pollution analysis system for complex terrain. J. Appl. Meteor., 30:909-923, 1991.
- D.G. Ross, G.S. Lorimer, J. Ciolek Jr., and D.G. Fox. Development and evaluation of a wind field model for emergency preparedness in complex terrain. In 86th Annual Meeting & Exibition, Denver, Colorado, JUNE 13 18 1993.
- 32. X. Guo and J.P. Palutikof. A study of two mass-consistent models: problems and possible solutions. Bound. Layer Meteorol., 53:303-332, 1990.
- 33. C.F. Ratto, R. Festa, O. Nicora, R. Mosiello, A. Ricci, D.P. Lalas, and O.A. Frumento. Wind field numerical simulations: a new user-friendly code. In W. Pals, editor, 1990 European Community Wind Energy Conference, 10-14 September, Madrid, Spain, pages 130 134, H. S. Stephens & Associates, 1990.
- 34. H. Ishikawa. Development of regionally extended/worldwide version of system for prediction of environmental emergency dose information: WSPEEDI, (I) application of mass-consistent wind field model to synoptic wind fields. J. Nucl. Sci. Technol., 28:535-546, 1991.
- 35. J. Moussafir. Reconstruction tridimensionelle d'un champ de vent dans un domaine a topographie complexe a partir de mesures in situ. Lecture given at the first Workshop on Modeling of the Atmospheric Flow Fields, ICTP, Trieste, May 1988. (Unpublished).
- R. Mathur and L.K. Peters. Adjustment of wind fields for application in air pollution modeling. Atmos. Environ., 24:1095-1106, 1990.

- Y. Sasaki. An objective analysis based on the variational method. *Journal Met. Soc. Japan*, 36:77
 –88, 1958.
- Y. Sasaki. Some basic formalism in numerical variational analysis. Monthly Weather Review, 98:875-883, 1970.
- J.C. Barnard, H.L. Wegley, and T.R. Hiester. Improving the performance of mass consistent numerical models using optimization techniques. J. Climate Appl. Meteor., 26:675-686, 1987.
- J.C. Barnard and A. Germain. Verification of the Optimizing NOABL Model using a spatially dense Wind Data Set. Technical Report, Battelle Memorial Institute, Pacific Northwest Laboratory, 1988.
- 41. I. Troen. The European Wind Atlas II: modelling of flow in complex terrain. In G. Bergebes and J. Chadjivassiliadis, editors, Delphi Workshop on Wind Energy Applications, 1985.
- D.G. Ross and I.N. Smith. Discussion: adjustment of wind fields for application in air pollution modeling. Atmos. Environ., 25A:2425-2426, 1991.
- Y. Takeuchi and T. Adachi. Seasonal variations of atmospheric trajectories arriving at Osaka in the Kansai area. Atmos. Environ., 24 A:2011-2018, 1990.
- 44. E.W. Georgieva. Meteorological aspects of wind energy utilization in Bulgaria. Numerical modelling of the wind field. PhD thesis, Bulgarian Academy of Science, Institute of Geophysics, Sophia, 1990. (In Bulgarian).
- J.C.R. Hunt and W.H. Snyder. Experiments on stably and neutrally stratified flow over a model three-dimensional hill. *Journal of Fluid Mechan*ics, 96:671-704, 1980.
- R. Röckle. Bestimmung der Strömungsverhältnisse im Bereich komplexer Bebauungsstrukturen. PhD thesis, Technical University of Darmstadt, 1990.
- W.S. Lowellen, R.I. Sykes, and D. Oliver. The evaluation of MATHEW/ADPIC as a real time dispersion model. Technical Report No 442, NUREG/CR 2199 ARAP, U.S. Nuclear Regulatory Comm., 1982.
- T. Kitada, K. Igarashi, and M. Owada. Numerical analysis of air pollution in a combined field of land/sea breeze and mountain/valley wind. J. Climate Appl. Meteor., 25:767-784, 1986.
- J. Moussafir. Wind field reconstruction techniques. Lecture given at the first Workshop on Modeling of the Atmospheric Flow Fields, ICTP, Trieste, May 1988. (Unpublished).
- 50. H.G. Parkinson. An assessment of the economic wind energy resource in the UK. In W. Pals, editor, Resource assessment. European Community Wind Energy Conference, H. S. Stephens & Associates, Madrid, 1990.
- 51. S.F. Burch and K. Newton. Computer modelling

- the UK Wind Energy Resource: Phase I Optimization of the Methodology. Technical Report ETSU WN 7053, Material Physics and Metallurgy Division Harwell Laboratory, 1992.
- 52. S.F. Burch, M. Makari, K. Newton, F. Ravenscroft, and J. Whittaker. Computer modelling the UK Wind Energy Resource: Phase II Application of the Methodology. Technical Report ETSU WN 7054, Material Physics and Metallurgy Division Harwell Laboratory, 1992.
- 53. A.M. Sempreviva, I. Troen, and A. Lavagnini. Modelling of wind power potential in Sardinia. In W. Palz and E. Sesto, editors, *Proceedings of EWEC'86*, European Wind Energy Association, A. Raguzz, Fome, Rome, 7-9 October 1986.
- 54. L. Adell, L. Zubiaur, F. Martin, F. Ferrando, P. Moreno, L. Varona, and A. Pantoja. Development of a methodology for the estimation of wind energy resources in relatively large areas: applications to the eastern and central part of Spain. Solar Energy, 38:281-295, 1987.
- 55. F. Boschetti, O.A. Frumento, and C.F. Ratto. Methodology and preliminary results of a study on the impact on air quality of an incinerator located in a complex orography. *Physica Medica*, IX:271 – 273, 1993.
- M. Bocciolone, M. Gasparetto, S. Lagomarsino, G. Piccardo, C.F. Ratto, and G. Solari. Statistical analysis of extreme wind speeds in the Straits of Messina. J. Wind Eng. Ind. Aerodyn., 48:359-377, 1993.
- 57. S.S. Zilitinkevich. Velocity profiles, the resistence law and the dissipation rate of mean flow kinetic energy in a neutrally and stably stratified planetary boundary layer. *Bound. Layer Meteorol.*, 46:367-387, 1989.
- 58. T.R. Hiester and W.T. Pennell. The meteorological aspects of siting large wind turbines. Battelle Memorial Institute, Pacific Northwest Laboratory, 1981.
- 59. V. Barros. Coupling a mass-consistent model with a non-stationary one-dimensional model. In D.P. Lalas and C.F. Ratto, editors, Modelling of Atmospheric Flow Fields. Lectures given at the International Centre for Theoretical Physics, Trieste, Italy, World Scientific Publishing Co. Ltd., 1994.
- 60. N. Moussiopoulos. The diagnostic wind model CONDOR. In D.P. Lalas and C.F. Ratto, editors, Modelling of Atmospheric Flow Fields. Lectures given at the International Centre for Theoretical Physics, Trieste, Italy, World Scientific Publishing Co. Ltd., 1994.
- Th. Flassak and N. Moussiopoulos. Direct solution of the Helmholtz equation using fourier analysis on scalar and vector computers. Environ. Software, 1988.
- 62. R.M. Traci, G.T. Phillips, and K.H. Rock. Wind

energy siting methodology - Windfield Model Verification Program I. Oahu, Hawaii, Data Set. Technical Report DOE/ET/20280-79/3., NTIS U.S. Dept. of Energy, Science Application Inc.. Springfield, Virginia, 1979.

o mars dal dis

J. 1980

10 8 AV

- 63. R.M. Traci, D.C. Wyatt, P.C. Patnaik, and Phillips. Wind energy siting methodology - Windfield Model Verification Program II. Nevada Test Site Data Set. Technical Report DOE/ET/20280-79/3, NTIS U.S. Dept. of Energy, Science Application Inc.., Springfield, Virginia, 1980.
- 64. P.J. Mason and J.C. King. Measurements and predictions of flow and turbulence over an isolated hill of moderate slope. Q. J. R. Meteorol. Soc., 111:617-640, 1985.
- W.H. Snyder. The EPA Meteorological Wind Tunnel: its Design, Construction and Operating Characteristics. U.S. Environmental Protection Agency, Research Triangle Park, N.C., 1976.
- F.L. Ludwig and G. Byrd. An efficient method for deriving mass-consistent flow fields from wind observations in rough terrain. Atmos. Environ., 14:585-587, 1980.